

SUPPLEMENTARY INFORMATION

Archaeal extracellular vesicles are produced in an ESCRT-dependent manner and promote gene transfer and nutrient cycling in extreme environments

Junfeng Liu^{1,2}, Virginija Cvirkaite-Krupovic², Pierre-Henri Commere³, Yunfeng Yang¹, Fan Zhou¹, Patrick Forterre², Yulong Shen¹, Mart Krupovic^{2*}

¹ CRISPR and Archaea Biology Research Center, State Key Laboratory of Microbial Technology, Microbial Technology Institute, Shandong University, Qingdao, China

² Archaeal Virology Unit, Institut Pasteur, 75015 Paris, France

³ Institut Pasteur, Flow Cytometry Platform, 75015 Paris, France

* – Correspondence to:

Mart Krupovic
Archaeal Virology Unit,
Department of Microbiology, Institut Pasteur,
75015 Paris, France
E-mail: mart.krupovic@pasteur.fr
Tel: 33 (0)1 40 61 37 22

Running title:

Role of extracellular vesicles in extreme environments

SUPPLEMENTARY METHODS

Cell cycle synchronization

S. islandicus cells were synchronized as previously described for *S. acidocaldarius* [1, 2], with some modifications. Specifically, Sis/pSeSD cells were first grown aerobically at 75°C with shaking (145 rpm) in 30 ml of STV medium. When the OD₆₀₀ reached 0.6-0.8, the cells were transferred into 300 ml MTSV medium with an initial OD₆₀₀ of 0.05. When the OD₆₀₀ reached 0.15-0.2, acetic acid (final concentration, 6 mM) was added into the cell culture for 6 h, resulting in cell cycle arrest at the end of the DNA synthesis phase (S phase). Then, the cells were pelleted down at 5,000 rpm for 15 min at room temperature to remove the acetic acid and washed once with 0.7% (wt/vol) sucrose. Finally, the cells were resuspended into 300 ml of the pre-warmed MTSV medium.

Detection of EVs in environmental samples

Hot spring water samples collected from the solfataric field of the Campi Flegrei volcano in Pozzuoli, Italy have been described previously [3]. Twelve milliliters of the sample were concentrated by ultracentrifugation at 38,000 rpm (SW41 rotor) at 15°C for 3 h. After centrifugation, most of the supernatant was removed and the pellet was resuspended in the residual liquid (~300 µl). The concentrated sample was prepared for TEM analysis as described above.

Cell cycle and cell size analysis by flow cytometry

The cell cycle of synchronized cells and the cell sizes of knockdown and over-expression strains were analyzed by flow cytometry. Around 0.6×10^8 cells were collected for flow cytometry analysis. Briefly, cells at indicated time points were pelleted at 6,000 rpm for 5 min, resuspended in 300 µl of PBS, and then 700 µl of cool ethanol were added for at least 12 h to fix the cells. The fixed cells were then pelleted at 2,800 rpm for 20 min and washed with 1 ml of PBS. Finally, the cells were pelleted and resuspended in 80 µl of staining buffer containing 40 µg/ml propidium iodide (PI). After staining for 30 min, the DNA content or cell sizes were analyzed using the ImageStreamX MarkII Quantitative imaging analysis flow cytometry (Merck Millipore, Germany), which was calibrated with non-labeled beads with a diameter of 2 µm. The data from analysis of at least 100,000 cells was collected from each sample and analyzed with the IDEAS data analysis software.

EV-mediated gene transfer

EVs isolated and purified from 6 L of exponentially growing Sis/pSeSD culture (24 h) were used for gene transfer experiments as described previously [4], with some modification. Briefly, E233S cells were grown in 30 ml of MTSVU medium until optical density reached 0.2 and then harvested by centrifugation (7,000 rpm for 10 min at room temperature). The cell pellet was washed 6 times with 30 ml of 0.7% (wt/vol) sucrose solution to remove the uracil and then resuspended in 30 ml of MCSV. One ml of EV preparation (76 µg/ml based on the total protein amount) or PBS (control) were added to 5 ml of E233S cell culture. The cells were incubated at 75°C with shaking (145 rpm). After 3 h, 5 h and 7 h of incubation 100 µl of each sample were collected and serial dilutions were spread on the pre-warmed MCSV plates and incubated at 75°C. After 10 days of incubation, single colonies were picked, inoculated into nuclease free water and 2 µl were used as template for PCR with plasmid-specific primers pSeSD-F and pSeSD-R (Table S5) to check for the presence of pSeSD plasmid.

Determination of the relative EV diameters

Due to pleomorphicity of EVs, their relative diameters were determined by measuring the corresponding area (A) using ImageJ. First, the electron micrographs of negatively stained EVs were opened in ImageJ and the scale of each image was set according to the scale bar in the corresponding micrograph. Then the area of each EV was measured separately and the relative diameter (D) was calculated according to the area, based on the equation $A = (\pi/4) \times D^2$.

Live/Dead staining and fluorescence microscopy analysis

Live/Dead staining was carried out using the LIVE/DEAD BacLight™ Bacterial Viability Kit (Invitrogen, US) [5, 6] according to the supplier's protocols. Specifically, around 0.6×10^8 cells from the cell cultures at indicated time points were pelleted at 6,000 rpm for 5 min and resuspended in 50 µl of the M (mineral salts) solution. Then, the cells were mixed with 50 µl of the 2X stock solution of the LIVE/DEAD BacLight staining reagent mixture giving the final concentrations of SYTO 9 and propidium iodide of 6 µM and 30 µM, respectively. The samples

were incubated at room temperature in the dark for 15 min, then the excess of dyes was removed by centrifugation at 6,000 for 5 min. The cells were resuspended in 80 μ l of the M solution and 5 μ l were used for fluorescence microscopy observation under the Leica TCS SP8 confocal microscope (Leica, Germany). The data was analyzed using the Leica Application Suite X imaging and analysis software (Leica, Germany).

For DAPI staining of the cells, around 0.6×10^8 cells from the cell cultures were pelleted at 6,000 rpm for 5 min and resuspended in 80 μ l of PBS staining buffer containing 9 μ M (2.5 μ g/ml) DAPI. For DAPI staining of the EVs, 50 μ l of EV preparations were mixed with the 2 \times DAPI stock solution, giving a final concentration of DAPI of 9 μ M (2.5 μ g/ml). After staining for 30 min, 5 μ l of DAPI-stained samples were used for fluorescence microscopy observation under the Leica TCS SP8 confocal microscope (Leica, Germany).

Mass spectrometry and data analysis

The total protein content (i.e., membrane-associated and soluble proteins) of the Sis/pSeSD cells and highly purified (see above) EVs were analyzed by tandem liquid chromatography–tandem mass spectrometry (LC-MS/MS). The EVs and cells were snap-frozen in liquid nitrogen, lyophilized and re-suspended in 100 μ l of lysis buffer including 8 M Guanidine HCl (GuHCl), 5 mM Tris(2-carboxyethyl)phosphine (TCEP) and 20 mM 2-chloro-acetamide (CAA). After kept at 95°C for 5 min, 900 μ l of 50 mM Tris-HCl (pH 8.0) were added to the samples to dilute GuHCl to a concentration of under 1M. Then a mixture of 500 ng of LysC/Trypsin was added to the samples and kept at 37°C overnight for digestion of the proteins. The reaction was stopped by addition of 1% formic acid. Peptides were desalted using Sep-Pac C18 Cartridges (Waters, USA), following the manufacturer's instructions. The purified peptides were concentrated to near dryness, re-suspended in 20 μ l of 0.1% formic acid and analyzed by Nano LC-MS/MS at the Proteomics Platform of Institut Pasteur (Paris, France) using an EASY-nLC 1200 system (peptides were loaded and separated on a 30 cm long home-made C18 column; Thermo Fisher Scientific, Waltham, MA, USA) coupled to a Q Exactive Plus system (Thermo Fisher Scientific) tuned to the DDA mode. Peptide masses were searched against annotated *S. islandicus* REY15A proteins using Andromeda with the MaxQuant ver. 1.3.0.543 244 software, and additionally with the X!Tandem search engine. Identified proteins were functionally annotated against the archaeal clusters of orthologous groups (arCOG) database [7].

Heterotrophic growth assay

EVs were isolated from 20 L of Sis/pSeSD cell culture and purified by ultracentrifugation in sucrose gradient as described above and resuspended in 18 ml of the M (mineral salts) solution. The final concentration of the EV preparation was 49.6 μ g/ml, based on the total protein amount. *S. islandicus* REY15A cells were cultured in MTSV medium and collected when they reached the early logarithmic phase ($OD_{600}=0.2$). The cells were washed 6 times with the M solution by centrifugation at 7,000 rpm for 10 min to remove the traces of sucrose (S) and tryptone (T). The washed cells were inoculated into 10 ml of MV, MSV and MTSV medium as the control groups, to the initial OD_{600} of 0.05. Experimental groups were each supplemented with 1.5 ml of the EV preparations containing different concentration of EVs (24.8 μ g for group I, 49.6 μ g for group II and 74.4 μ g for group III). The experiment was repeated three times.

Construction of the CRISPR type III-B-based RNA interference plasmids and RNA interference

The CRISPR type III-B-based RNA interference plasmids were constructed according to the methods described previously [8, 9]. For RNA interference, 40-nt protospacers matching the genes of interest were selected from the anti-sense strand of the corresponding genes downstream of the GAAAG, CAGAG or AAAG (5'-3') sequences and cloned into the genome-editing plasmid pGE [8]. The spacers selected and used in this study are listed in Table S4. Spacer fragments were generated by annealing the corresponding complementary oligonucleotides and inserted into pGE at the BspMI restriction site. Plasmid pGE was introduced into E233S cells by electroporation and transformants were selected on MSCV plates without uracil. RNA interference was induced by arabinose (0.2% wt/vol final concentration). For enumeration with flow cytometry, the EVs were collected from 50 ml of cell cultures during the exponential growth phase of different knockdown strains (24 h), as described above. The flow cytometry measurements were done in triplicate (Fig. S16).

RNA preparation and quantitative reverse-transcription PCR (RT-qPCR)

Cells from RNA interference (knockdown) strains were collected for RNA extraction after 24 h post induction. Total RNAs were extracted using TRI Reagent® (SIGMA-Aldrich, USA). The concentrations of the total RNAs

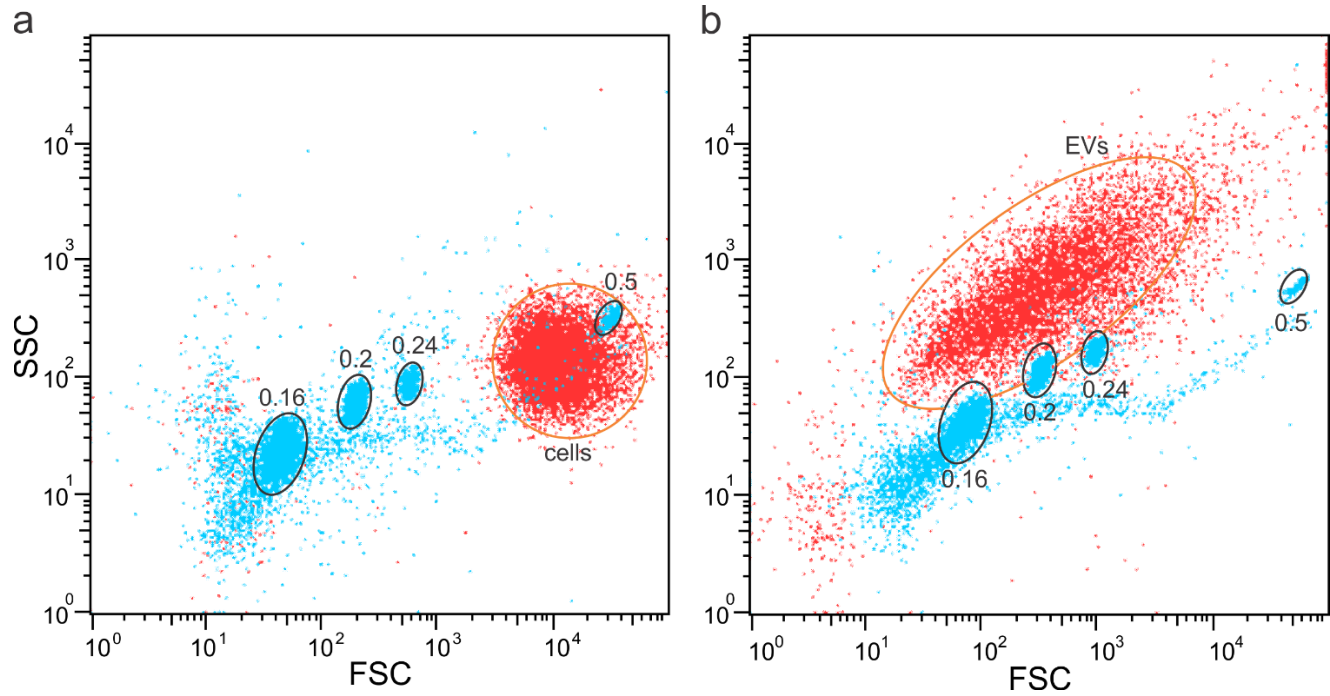
were estimated using the Eppendorf BioSpectrometer® basic (Eppendorf AG, Germany). The quality of the RNA preparations was further checked by agarose gel electrophoresis.

First-strand cDNAs were synthesized from the total RNAs according to the protocol of Maxima First Strand cDNA Synthesis Kit for RT-qPCR with dsDNase (Thermo Scientific, USA). Shortly, 2 µg of RNA were treated with the dsDNAase at 37°C and then the reverse transcription reaction was carried out by incubation for 10 min at 25°C followed by 30 min at 50°C, and finally terminated by heating at 85°C for 5 min. The resulting cDNA preparations were used to evaluate the mRNA levels of the targeted genes by qPCR (2ng of cDNA were used as the template), using Luna® Universal qPCR Master Mix (New England Biolabs, USA) and gene-specific primers (Table S5). qPCR was performed in an Eppendorf MasterCycler RealPlex⁴ (Eppendorf AG, Germany) with the following steps: denaturing at 95°C for 2 min, 40 cycles of 95°C 15 s, 55°C 15 s and 68°C 20 s. Relative amounts of mRNAs were calculated using the comparative Ct method with 16S rRNA as the reference [10]. Three independent biological experiments and three technical replicates were carried out for RT-qPCR.

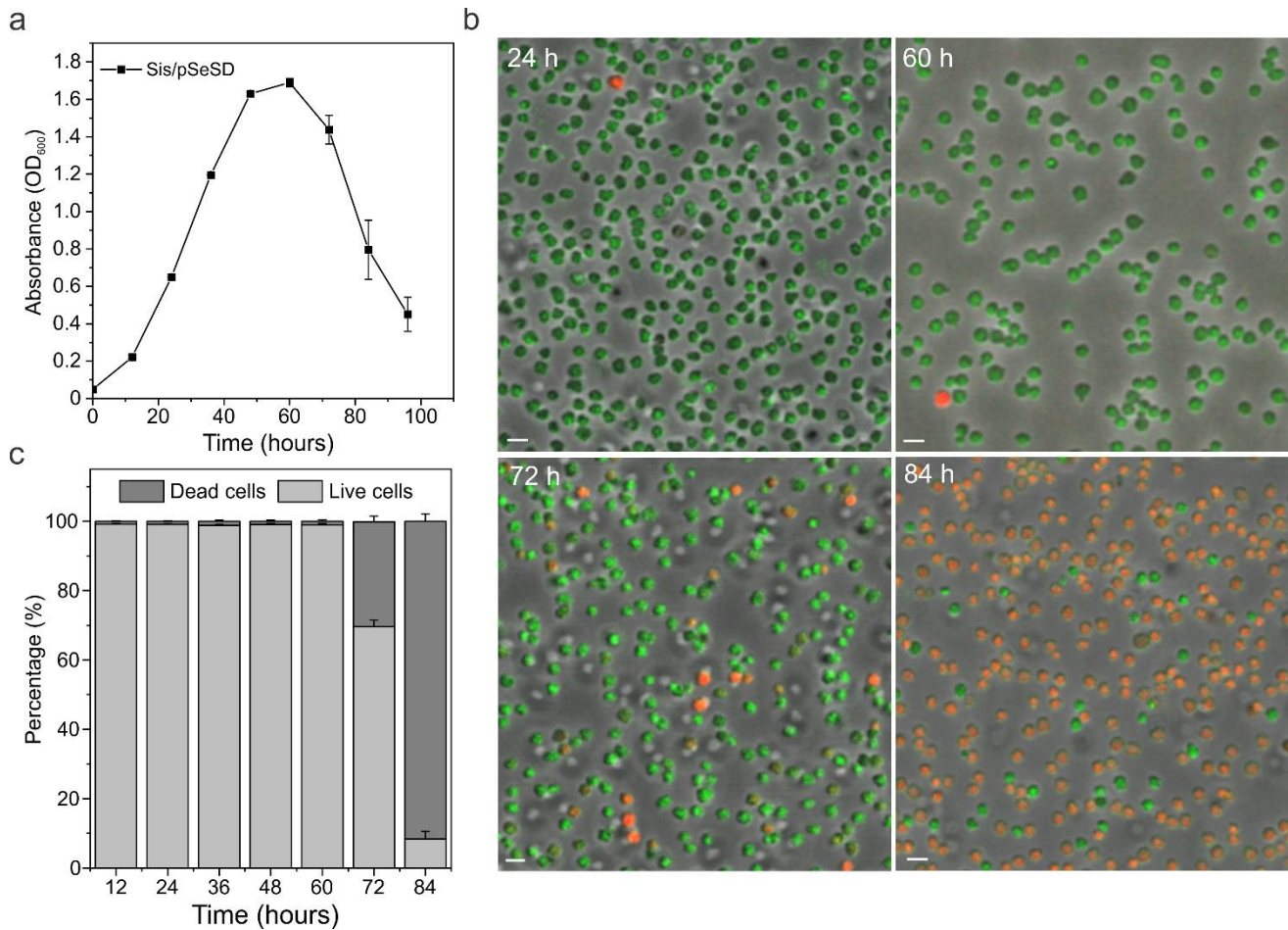
Western blot

To verify the presence of ESCRT proteins in the EVs, the sucrose-gradient purified EV samples were run in 12% polyacrylamide gel using tris-glycine running buffer, then transferred onto PVDF membrane. ESCRT proteins were detected using antibodies against ESCRT-III, ESCRT-III-1 and ESCRT-III-2 (HuaAn Biotechnology Co., Hangzhou, Zhejiang, China), as described previously [11]. The goat anti-rabbit (Thermo Fisher Scientific, USA) secondary antibodies coupled with peroxidase were used as secondary antibodies. The specific bands were detected by chemoluminescence using ECL prime western blotting detection reagents (Amersham) according to the manufacturer's instructions. Proteins purified from *E. coli* BL21-CodonPlus(DE3)-RIL (Agilent Technologies) were used as the positive controls.

SUPPLEMENTARY FIGURES

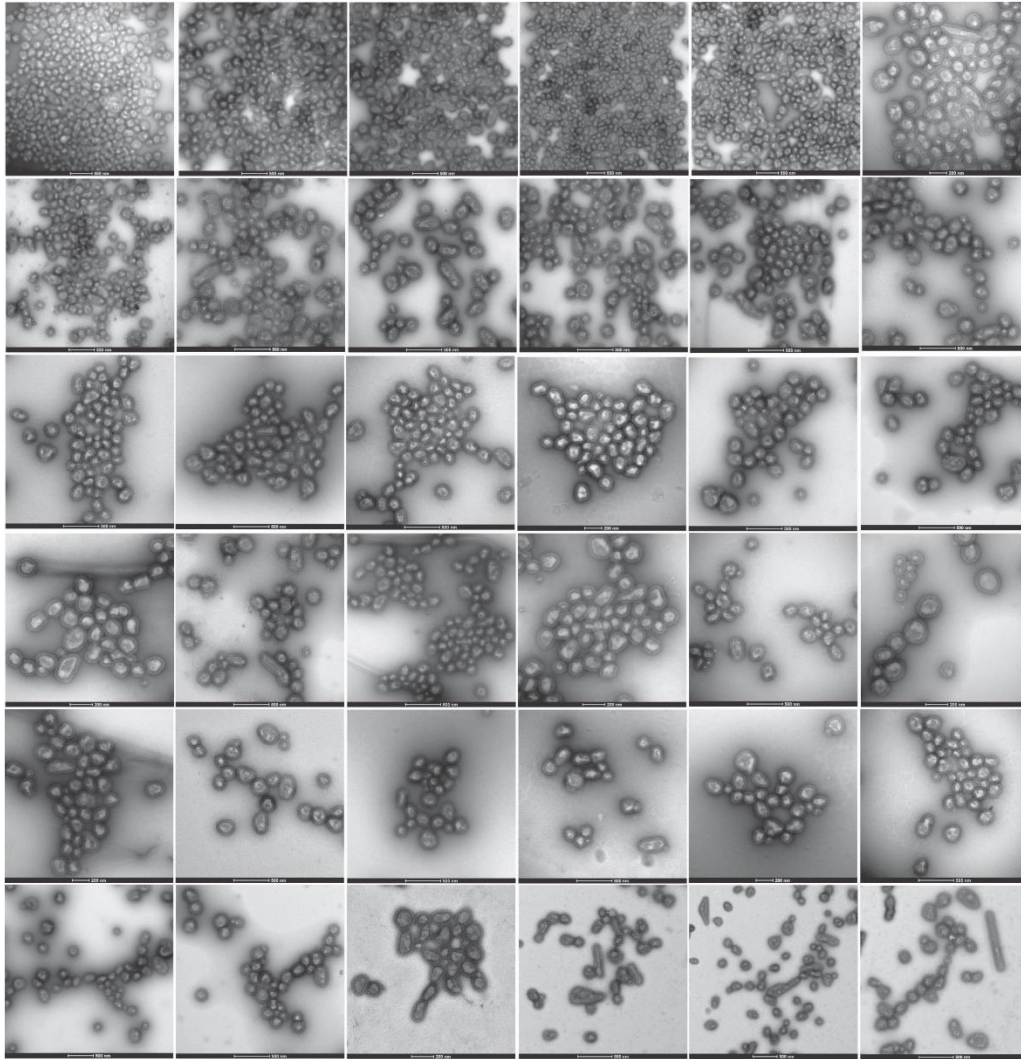


Supplementary Fig. 1. Quantification of the number of EVs by flow cytometry. **a** *S. islandicus* cells carrying pSeSD vector mixed with fluorescently-labeled beads of defined diameters (0.16-0.5 μm). **b** EV preparation mixed with beads of defined diameters (0.16-0.5 μm). Populations of cells and EVs are circled for convenience. The numbers indicate the diameter of the beads used in the flow cytometry analysis. SSC, side scattered light; FSC, forward scattered light.

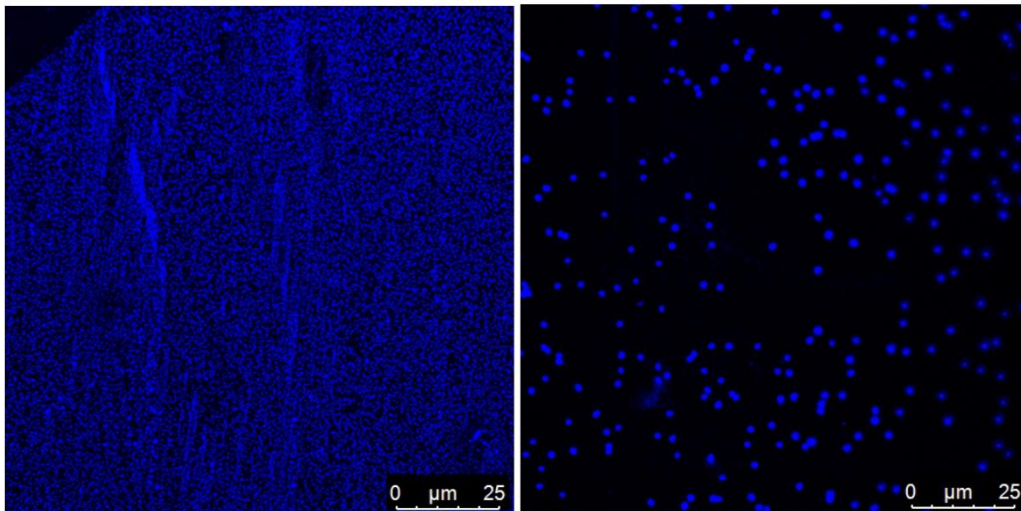


Supplementary Fig. 2. Live/dead staining of cells of Sis/pSeSD at different time points. **a** Growth curve of Sis/pSeSD. Error bars represent standard deviation from three independent experiments. **b** Ratios of live and dead cells in the population estimated using live/dead staining of Sis/pSeSD cells at different time points. Error bars represent standard deviation from three independent experiments. Around 10,000 cells were counted for each experiment at each time point to calculate the ratio between live and dead cells. **c** Representative images of the live/dead staining of Sis/pSeSD cells at indicated time points. Scale bars, 2 μ m.

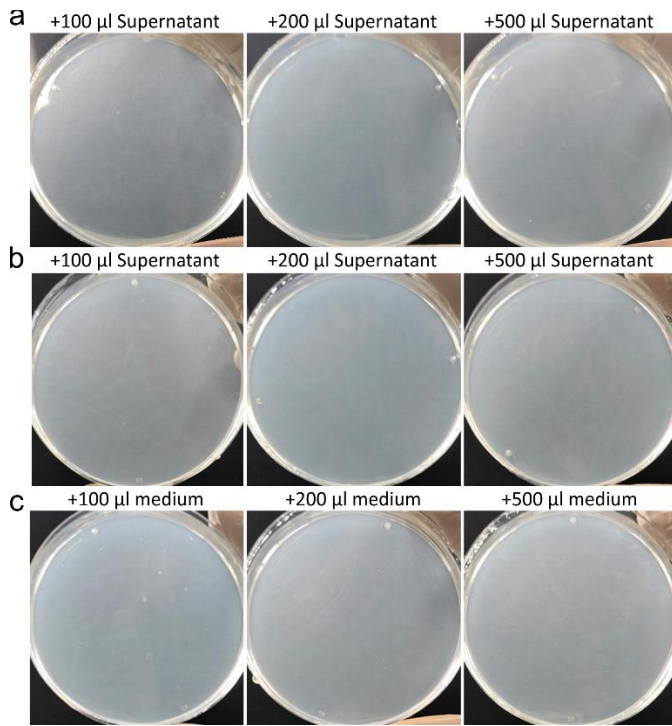
a



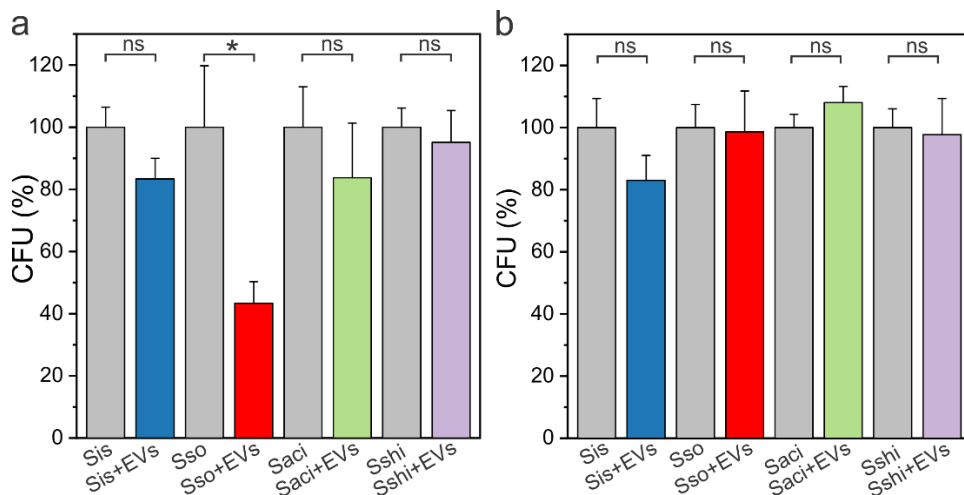
b



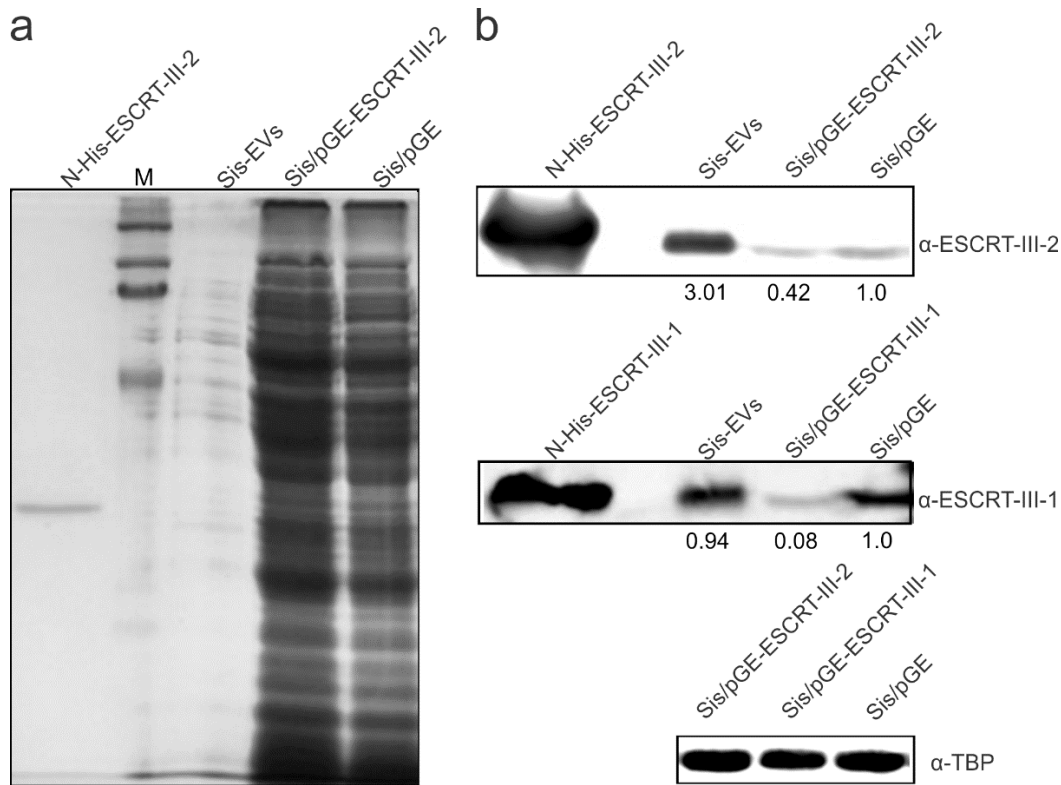
Supplementary Fig. 3. Evaluation of cellular contamination in Sis-EV preparations. **a** Thirty-six randomly acquired transmission electron micrograph of negatively stained Sis-EVs showing absence of cellular contaminants. Scale bars are shown below each micrograph. **b** Sis-EV preparation (left) and *S. islandicus* cells (right) stained with DAPI and observed under fluorescence microscope using the same magnification.



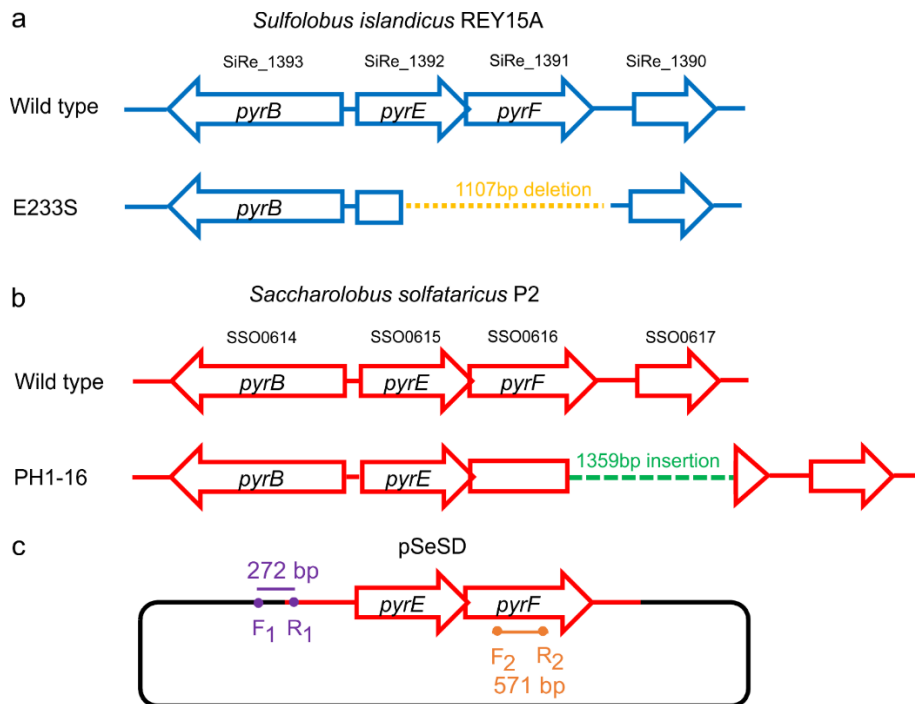
Supplementary Fig. 4. EVs do not form colonies on the plates. To evaluate the presence of cellular contaminants in the EV preparations, cell cultures of *Sulfolobus islandicus* E233S carrying pSeSD (a) or pSeSD-CdvA (b) plasmids were collected following induction with 0.2% (w/v) arabinose for 24 h, and centrifuged (7,000 rpm, 10 min, room temperature) to remove the majority of the cells. The supernatants were then filtered through 0.45 µm filter to remove the remaining cells and cell debris. Finally, 500 µl, 200 µl and 100µl of the filtered supernatants were spread on MCSV plates respectively and incubated at 75 °C. Same volumes of medium (c) were used as a control. After 10 days of incubation, no colonies formed on either of the plates, indicating that there were no cells in the filtered supernatants, whereas the large vesicles produced by the CdvA overexpression strain were not mini-cells.



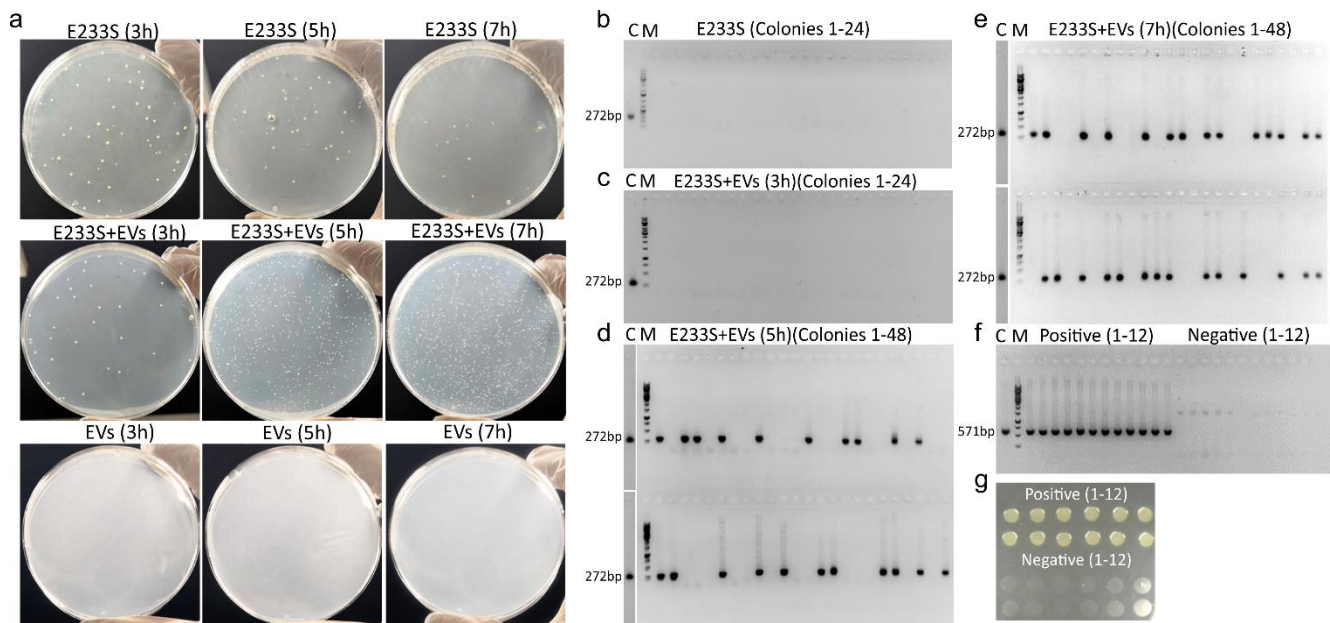
Supplementary Fig. 5. Effect of Sis-EVs on the ability of different *Sulfolobus* strains to form colonies. Sis-EVs produced by Sis/pSeSD strain were mixed with the cells, incubated for 3 (a) and 5 (b) hours and plated on rich medium. Star indicates significant difference based on the paired two-tailed t-test, $p=0.02907$. Error bars represent standard deviation from three independent experiments. Abbreviations: ns, non-significant; Sjs, *S. islandicus*; Sso, *S. solfataricus*; Saci, *S. acidocaldarius*; Sshi, *S. shibatae*.



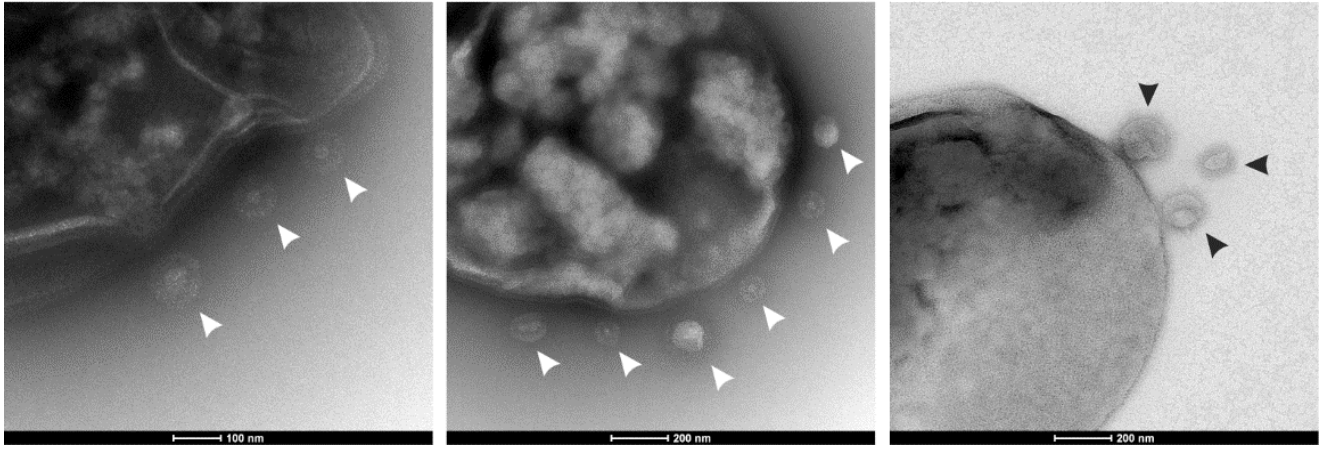
Supplementary Fig. 6. Confirmation of ESCRT-III-1 and ESCRT-III-2 presence in the Sis-EVs by western blot. ESCRT-III-2 and ESCRT-III-1 were highly enriched in Sis-EVs. **a** Coomassie blue staining of the protein gel. A total amount of 2.3 μ g of Sis-EV preparation and 0.75 mg of cells from the knockdown strain of *escrt-III-2* (Sis/pGE-ESCRT-III-2) and the cells with the empty vector (Sis/pGE) were loaded in the gel. **b** Western blot analysis of the amount of ESCRT-III-2 (top) and ESCRT-III-1 (bottom) in Sis-EVs as well as in the corresponding knockdown and control cells. N-His-ESCRT-III-2 and N-His-ESCRT-III-1 are proteins purified from the *E. coli* cells that were used as the positive controls. Anti-TBP antibodies were used as the loading control.



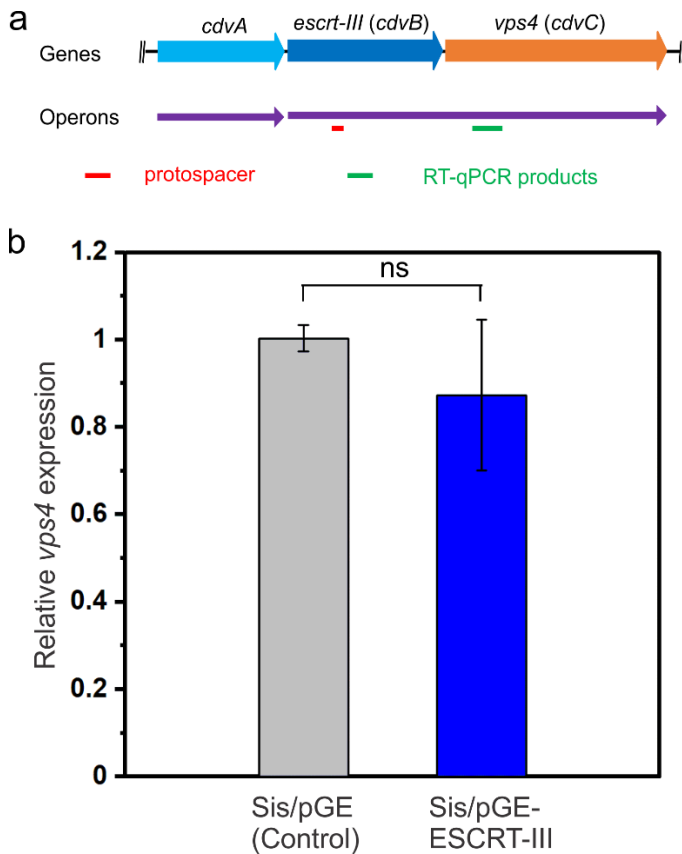
Supplementary Fig. 7. Schematic showing the genotypes of the uracil auxotroph mutants of *S. islandicus* REY15A (E233S) and *S. solfataricus* P2 (PH1-16). **a** E233S is a uracil auxotroph mutant of *S. islandicus* REY15A, carrying a 1107bp deletion including the 3'-distal 233bp of the *pyrE* gene and the entire *pyrF* gene [12]. **b** The *pyrEF* locus in the genome of *S. solfataricus* P2 and PH1-16. The latter carries a transposon insertion (1359 bp) within the *pyrF* gene [13]. **c** pSeSD is an *E. coli-Sulfolobus* shuttle vector. It contains *pyrEF* genes and their adjacent regions originating from *S. solfataricus* P2. When electroporated into E233S cells, pSeSD restores the ability of E233S cells to synthesize uracil. F1 and R1 (in purple) are the forward and reverse primers targeting the pSeSD multiple-cloning site and the adjacent region, including the arabinose-inducible promoter, start codon and terminator. F2 and R2 (in orange) are the forward and reverse primers targeting a fragment of the pSeSD *pyrF* gene. The two sets of primers were used to confirm the transfer of pSeSD plasmid into E233S cells (see Figures 3d and S8).



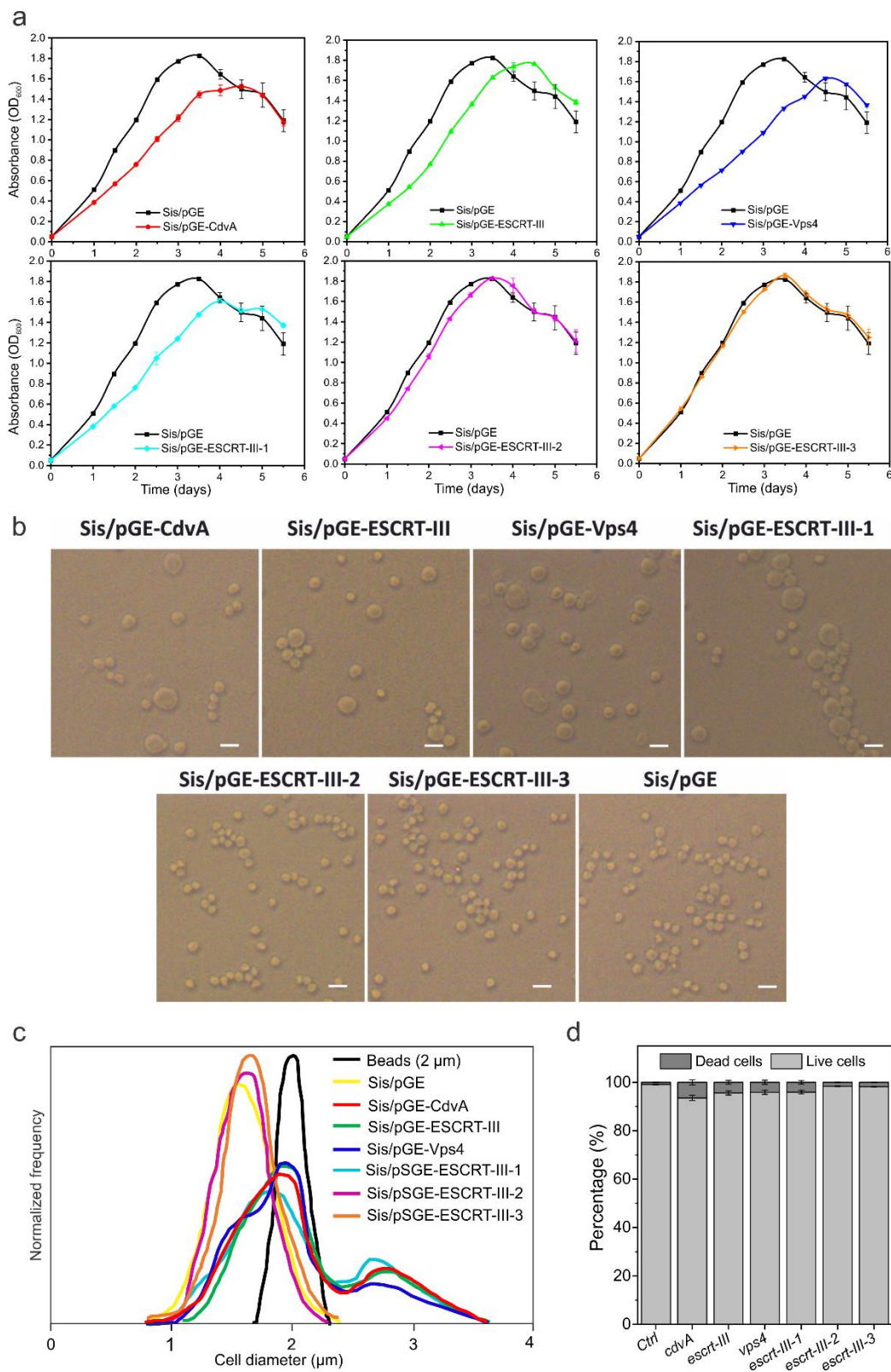
Supplementary Fig. 8. Gene transfer by Sis-EVs. **a** Representative plates showing colony formation of uracil auxotroph strain E233S without incubation with Sis-EVs (top) and after incubation with Sis-EVs for indicated time periods (middle). The bottom panel shows that no colonies were formed when purified Sis-EVs alone were plated on the uracil free plates. **b-e** PCR verification of the presence of pSeSD plasmid in the colonies described in panel **a** with the F1 and R1 primers (Fig. S6). **f** PCR verification of the *pyrF* gene presence in the isolated *S. islandicus* colonies with the F2 and R2 primers (Fig. S6). *pyrF* gene was present only in pSeSD-carrying colonies (positive 1-12); no ectopic *pyrF* integration in pSeSD-negative colonies (negative 1-12) was detected. Primer sequences used for PCR are provided in Table S5. **g** pSeSD-carrying (top 12) and pSeSD-negative (bottom 12) strains were spotted on MCSV plates without uracil; only pSeSD-carrying strains could stably grow. Abbreviations: C, positive control using pSeSD as a template (272 bp in panels b-e, primers F1-R1; 571 bp in panel f, primers R2-F2); M, size marker.



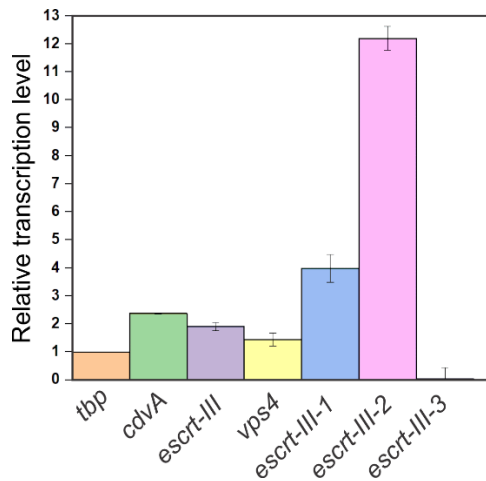
Supplementary Fig. 9. Transmission electron micrographs showing S-layer-coated EVs directly in the environmental sample. EVs are indicated with arrowheads. Scale bars are shown at the bottom of each image.



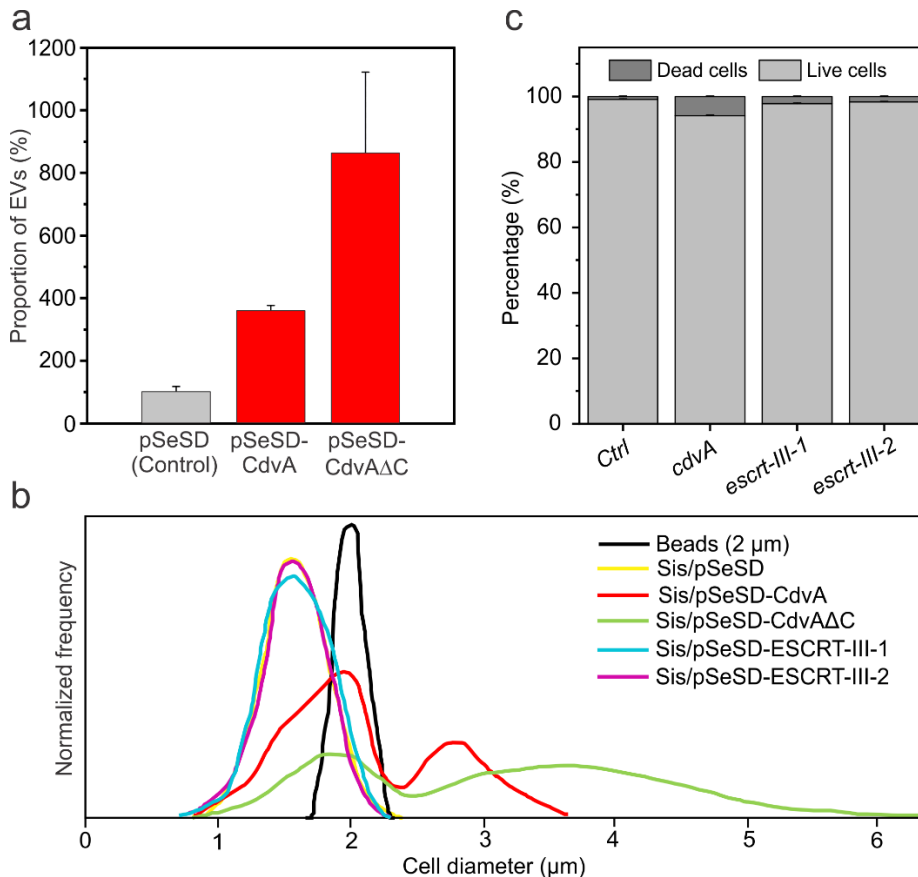
Supplementary Fig. 10. Gene silencing of *esct-III (cdvB)* does not affect the expression of the *vps4*. **a** Schematic showing the gene organization of the *Sulfolobus cdv* locus, containing *cdvA*, *esct-III (cdvB)* and *vps4 (cdvC)* genes. *esct-III* and *vps4* form a bicistronic operon [14, 15]. The location of the protospacer selected for the *esct-III* knockdown strain in this study is indicated with a red line, whereas the region amplified for the RT-qPCR analysis of the *vps4* is indicated with a green line. **b** Determination of the relative expression level of *vps4* in the control (Sis/pGE) and *esct-III* knockdown (Sis/pGE-ESCRT-III) strains by RT-qPCR. There was no significant difference of *vps4* expression in *esct-III* knockdown strain comparing with the control strain. The significance was evaluated using the paired two-tailed t-test, $p=0.2811$. ns, non-significant. Error bars represent standard deviation from three independent experiments.



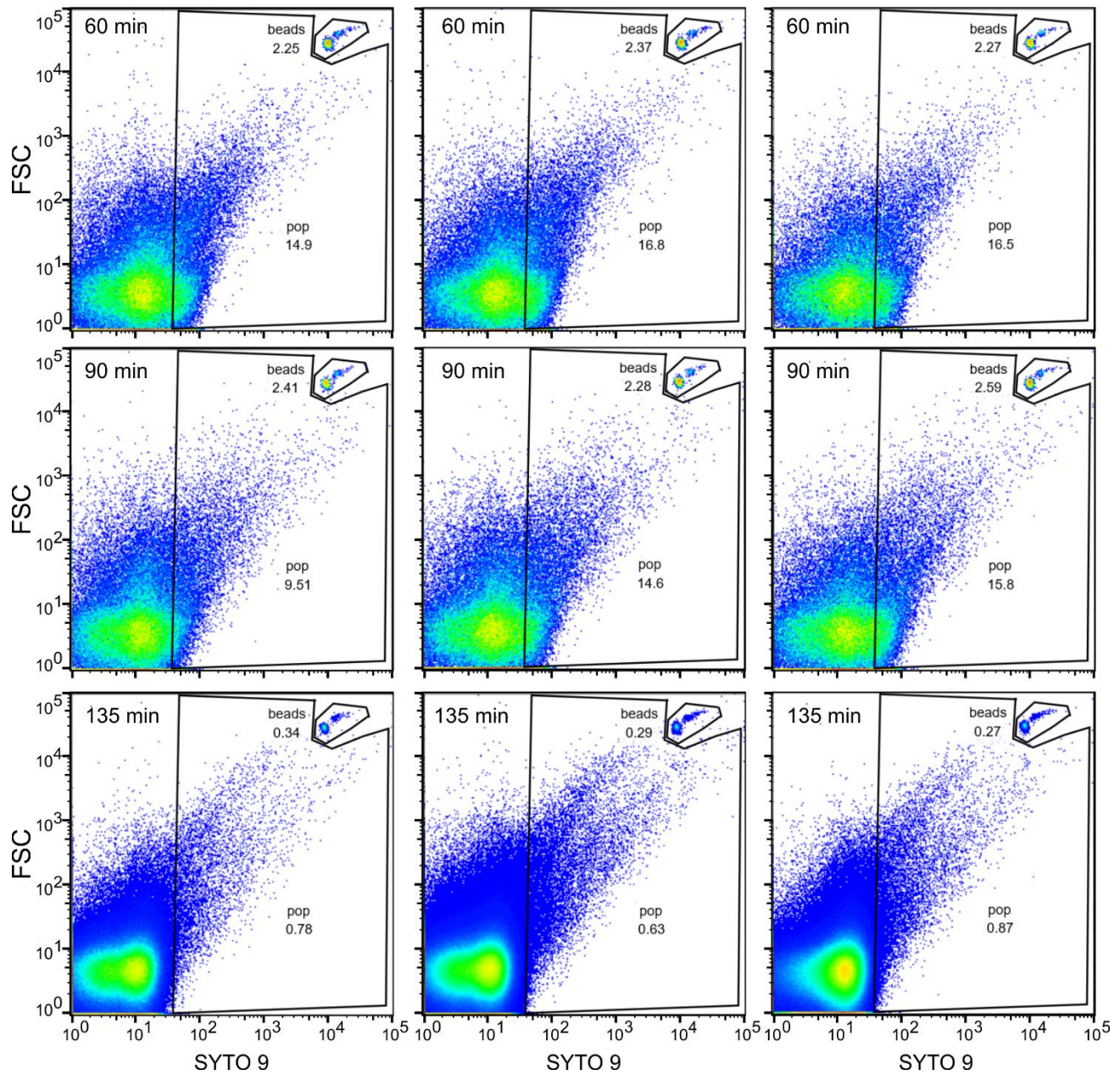
Supplementary Fig. 11. Characterization of the knockdown strains. **a** Growth curves of the knockdown strains. **b** Phase contrast micrographs of ESCRT knockdown strains. Bars, 2 μm . Strains containing an empty vector pGE were used as a negative control. **c** Cell size distribution in the knockdown cultures. Cell sizes were determined using flow cytometry as described in Materials and Methods. **d** Ratio of live and dead cells in the knockdown cultures.



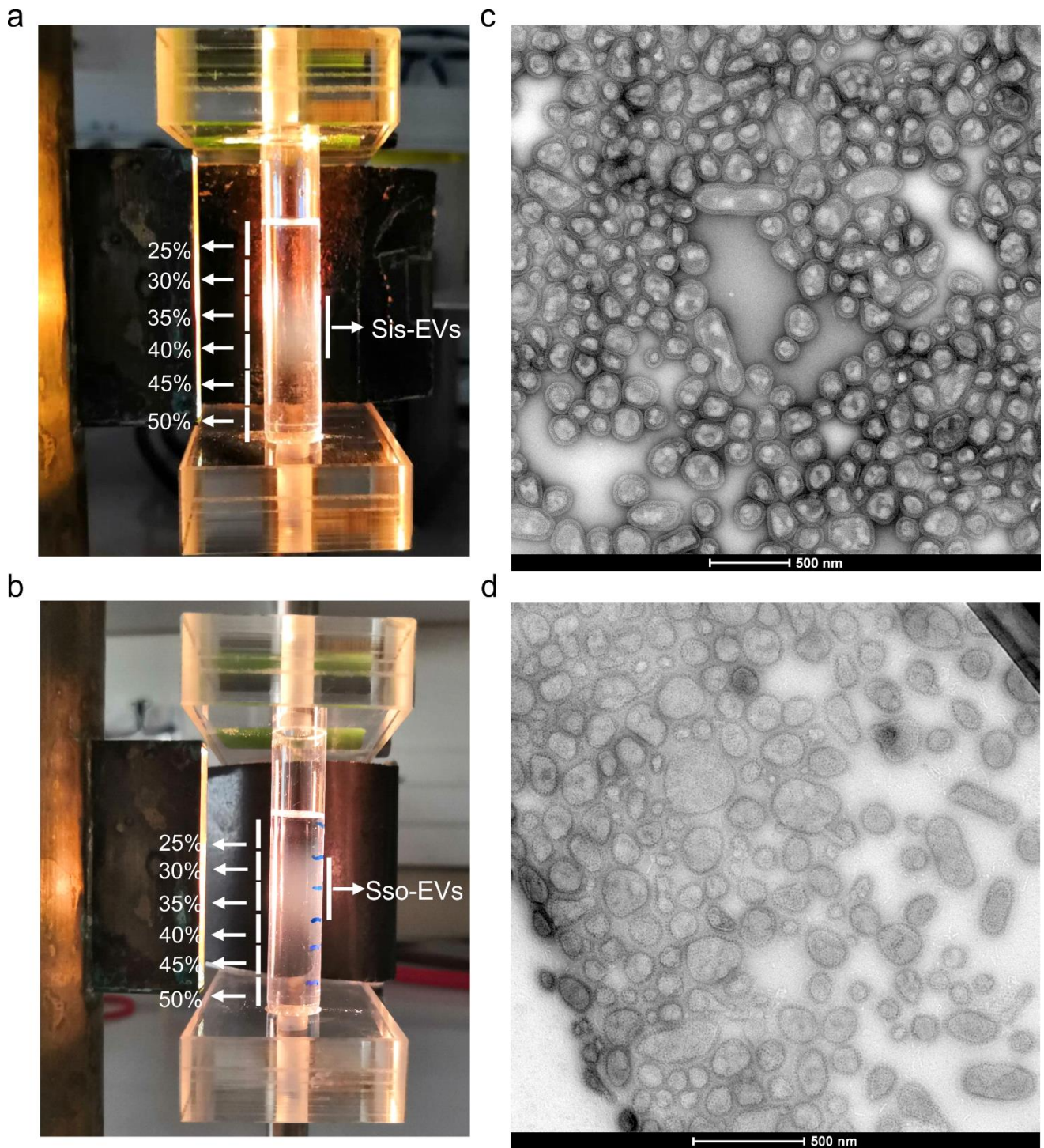
Supplementary Fig. 12. The relative expression of *escrt-III-2* is several times higher compared to other cell division genes in *S. islandicus* REY15A. For visualization purposes, the expression level of the housekeeping gene encoding TATA-binding proteins (TBP) is considered as unity, with the expression levels of all other genes calculated relative to TBP. Error bars represent standard deviation from three independent experiments.



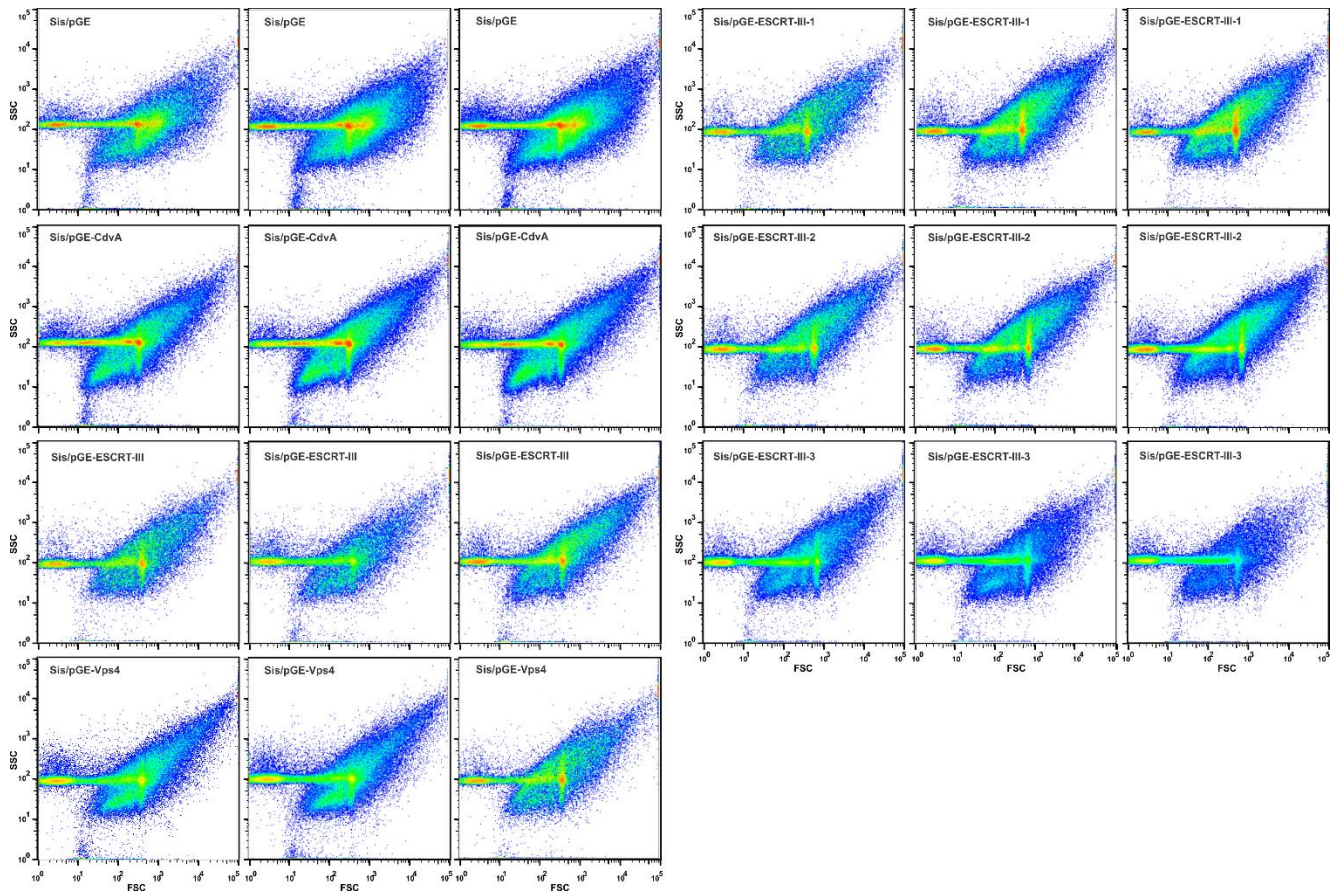
Supplementary Fig. 13. Characterization of EVs and *S. islandicus* cells overexpressing different ESCRT machinery components. **a** Quantification of the Sis-EVs released from the cells overexpressing CdvA and its C-terminally truncated mutant CdvA Δ C. Error bars represent standard deviation from three independent experiments. **b** Cell size distribution in *S. islandicus* cultures overexpressing different cell division proteins. Cell sizes were determined using flow cytometry as described in Materials and Methods. **c** Ratio of live and dead cells in the overexpression cultures.



Supplementary Fig. 14. Flow cytometry profiles of EV enumeration for synchronized Sis/pSeSD culture at different time points after removal of acetic acid. Three replicates are shown for each time point. The signal coming from the DNA-containing (SYTO9-positive) EVs is outlined. FSC, forward scattering.



Supplementary Fig. 15. EV purification by ultracentrifugation in sucrose gradient. EVs from *S. islandicus* (a) and *S. solfataricus* (b) formed opalescent bands in the 25-50% sucrose gradients in the region corresponding to 30%-40% sucrose. Transmission electron micrograph of negatively stained Sis-EVs (c) and Sso-EVs (d) collected from the corresponding opalescent bands. Scale bars, 500 nm.



Supplementary Fig. 16. Flow cytometry profiles of EV enumeration for different knockdown strains. Three replicates are shown for each strain. FSC, forward scattering; SSC, side scattering.

SUPPLEMENTARY TABLES

Table S1 Functional annotation of arCOG categories

arCOG category	Annotation
1. Information storage and processing	
J	Translation, ribosomal structure and biogenesis
A	RNA processing and modification
K	Transcription
L	Replication, recombination and repair
B	Chromatin structure and dynamics
2. Cellular processes and signaling	
D	Cell cycle control, cell division, chromosome partitioning
Y	Nuclear structure
V	Defense mechanisms
T	Signal transduction mechanisms
M	Cell wall/membrane/envelope biogenesis
N	Cell motility
Z	Cytoskeleton
W	Extracellular structures
U	Intracellular trafficking, secretion, and vesicular transport
O	Posttranslational modification, protein turnover, chaperones
X	Mobilome: prophages, transposons
3. Metabolism	
C	Energy production and conversion
G	Carbohydrate transport and metabolism
E	Amino acid transport and metabolism
F	Nucleotide transport and metabolism
H	Coenzyme transport and metabolism
I	Lipid transport and metabolism
P	Inorganic ion transport and metabolism
Q	Secondary metabolites biosynthesis, transport and catabolism
4. Poorly characterized	
R	General function prediction only
S	Function unknown

Table S2 Plasmids used in this study

Plasmid	Description	Reference
pSeSD	Empty vector for overexpression	[16]
pSeSD-CdvA	CdvA overexpression	[11]
pSeSD-CdvA Δ C	CdvA Δ C overexpression	[11]
pSeSD-ESCRT-III	ESCRT-III overexpression	[11]
pSeSD-ESCRT-III-1	ESCRT-III-1 overexpression	[11]
pSeSD-ESCRT-III-2	ESCRT-III-2 overexpression	[11]
pSeSD-ESCRT-III-3	ESCRT-III-3 overexpression	[11]
pGE	Empty vector for knockdown	[8]
pSeSD-Vps4	Vps4 overexpression	This study
pGE-CdvA	<i>cdvA</i> knockdown	This study
pGE-ESCRT-III	<i>escrt-III</i> knockdown	This study
pGE-Vps4	<i>Vps4</i> knockdown	This study

pGE-ESCRT-III-1	<i>escrt-III-1</i> knockdown	This study
pGE-ESCRT-III-2	<i>escrt-III-2</i> knockdown	This study
pGE-ESCRT-III-3	<i>escrt-III-3</i> knockdown	This study

Table S3 *Sulfolobus* strains used in this study

Strain	Phenotype	Reference
<i>S. solfataricus</i> PH1	<i>lacS:ISC1217</i>	[13]
<i>S. solfataricus</i> PH1-16	<i>pyrF:ISC1359, lacS:ISC1217</i>	[13]
<i>S. acidocaldarius</i> DSM 639	Wild type	[17]
<i>S. shibatae</i>	Wild type	[18]
<i>S. islandicus</i> REY15A	Wide type	[19]
Sis E233S	REY15A Δ <i>pyrEFAlacS</i>	[12]
Sis/pSeSD	Control for overexpression	[11]
Sis/pSeSD-CdvA	CdvA overexpression	[11]
Sis/pSeSD-CdvA Δ C	CdvA Δ C overexpression	[11]
Sis/pSeSD-ESCRT-III	ESCRT-III overexpression	[11]
Sis/pSeSD-ESCRT-III-1	ESCRT-III-1 overexpression	[11]
Sis/pSeSD-ESCRT-III-2	ESCRT-III-2 overexpression	[11]
Sis/pSeSD-ESCRT-III-3	ESCRT-III-3 overexpression	[11]
Sis/pSeSD-Vps4	Vps4 overexpression	This study

Table S4 Oligonucleotides used to construct knockdown plasmids

Name	Sequence (5'-3')	Source
CdvA-S-F	<u>AAGGCTTAAGTTCTATAGATTCTTTATCCAACGAGTCTAATCT</u>	This study
CdvA-S-R	<u>AGCAGATTAGACTCGTTGGATAAAGAATCTATAGAACTTAAGC</u>	This study
ESCRT-III-S-F	<u>AAGAAACGCCTTGCAGTTCTTGTACGGTATCTAGTTTTAGTCT</u>	This study
ESCRT-III-S-R	<u>AGCAGACTAAAAGTACGATACCGTACAAGAAGTCAAGGCGTTT</u>	This study
Vps4-S-F	<u>AAGTCCTGGAGTGTAATTGTTCTTGGTTACCTAAATTATTCT</u>	This study
Vps4-S-R	<u>AGCAGAATAATTTAGGTGAACCAAGAACAATTACACTCCAGGA</u>	This study
ESCRT-III-1-S-F	<u>AAGGCTCCTTAGAACCCTTTATTTTAAATCTCTCCTGCTCATA</u>	This study
ESCRT-III-1-S-R	<u>AGCTATGAGCAGGAGAGATTTAAAATAAAGGGTTCTAAGGAGC</u>	This study
ESCRT-III-2-S-F	<u>AAGTCCCCTGCTTCTATTACTACCTCTTGTAATCCCTCCTCTA</u>	This study
ESCRT-III-2-S-R	<u>AGCTAGAGGAGGGATTACAAGAGGTAGTAATAGAAGCAGGGGA</u>	This study
ESCRT-III-3-S-F	<u>AAGACATAATTATAAGTGCCTAACTTATTCTGCATTCTATTAA</u>	This study
ESCRT-III-3-S-R	<u>AGCTTAATAGAATGCAGAATAAGTTAGGCACTTATAATTATGT</u>	This study

Sequences added to the spacers for insertion into the BspMI restriction site of the genome editing plasmid pGE are underlined.

Table S5 Oligonucleotides used in this study

Name	Sequence (5'-3')	Source
16S-F	GAATGGGGGTGATACTGTCG	[20]
16S-R	TTTACAGCCGGGACTACAGG	[20]
ESCRT-III-F	CAGCATTCTTAGCTATTGAGAAAG	This study
ESCRT-III-R	GATAGAGTCTAAGGCTATTGC	This study
Vps4-F	GGATATAGTTCAAGCTGCACA	This study
Vps4-R	GATTAACACTTGGCATTCTGAC	This study
ESCRT-III-1-F	CGGAAAAGATTTCCAAAAGATTTG	This study
ESCRT-III-1-R	CAAGCCTACTAATCATGGAGC	This study
ESCRT-III-2-F	CGATGAAAGGAGTTATGCCAG	This study
ESCRT-III-2-R	CTTCTAATATCTTCCTTGCCTC	This study
ESCRT-III-3-F	GCTGAGCTGCTAATAGACG	This study
ESCRT-III-3-R	CTCAGACTCTCTAGCAACC	This study
Vps4-F-Nde I	GCGG <u>CATATG</u> AGTGCTCAAGTAATGCTAG	This study
Vps4-R-Sal I	TCACG <u>TCGACT</u> AATGCCTTAAACTTCTCT	This study
pSeSD-F	GCAATGTTAAACAAGTTAGGTATAC	This study
pSeSD-R	ACCTTATGTTAAACTACGCCAGT	This study
F1	CTGAGGCAGTCGAAGGATAG	This study
R1	TCGCTCTTTGCCTCACCTTG	This study
F2 (<i>pyrF</i> -F)	GCAATGGATAAACCTCTCTC	This study
R2 (<i>pyrF</i> -R)	CTGTTAATGGATTCCCTGCA	This study

SUPPLEMENTARY REFERENCES

1. Tarrason Risa G, Hurtig F, Bray S, Hafner AE, Harker-Kirschneck L, Faull P *et al.* The proteasome controls ESCRT-III-mediated cell division in an archaeon. *Science*. 2020; 369.
2. Lundgren M, Andersson A, Chen L, Nilsson P, Bernander R. Three replication origins in *Sulfolobus* species: synchronous initiation of chromosome replication and asynchronous termination. *Proc Natl Acad Sci U S A*. 2004; 101:7046-51.
3. Baquero DP, Contursi P, Piochi M, Bartolucci S, Liu Y, Cvirkaite-Krupovic V *et al.* New virus isolates from Italian hydrothermal environments underscore the biogeographic pattern in archaeal virus communities. *ISME J*. 2020; 14:1821-1833.
4. Tran F, Boedicker JQ. Plasmid characteristics modulate the propensity of gene exchange in bacterial vesicles. *J Bacteriol*. 2019; 201:e00430-18.
5. Robertson J, McGoverin C, Vanholsbeeck F, Swift S. Optimisation of the protocol for the LIVE/DEAD((R)) BacLight(TM) bacterial viability kit for rapid determination of bacterial load. *Front Microbiol*. 2019; 10:801.
6. Leuko S, Legat A, Fendrihan S, Stan-Lotter H. Evaluation of the LIVE/DEAD BacLight kit for detection of extremophilic archaea and visualization of microorganisms in environmental hypersaline samples. *Appl Environ Microbiol*. 2004; 70:6884-6.
7. Makarova KS, Wolf YI, Koonin EV. Archaeal Clusters of Orthologous Genes (arCOGs): An update and application for analysis of shared features between Thermococcales, Methanococcales, and Methanobacteriales. *Life (Basel)*. 2015; 5:818-40.
8. Li Y, Pan S, Zhang Y, Ren M, Feng M, Peng N *et al.* Harnessing Type I and Type III CRISPR-Cas systems for genome editing. *Nucleic Acids Res*. 2016; 44:e34.
9. Peng W, Feng M, Feng X, Liang YX, She Q. An archaeal CRISPR type III-B system exhibiting distinctive RNA targeting features and mediating dual RNA and DNA interference. *Nucleic Acids Res*. 2015; 43:406-17.
10. Schmittgen TD, Livak KJ. Analyzing real-time PCR data by the comparative C(T) method. *Nat Protoc*. 2008; 3:1101-8.
11. Liu J, Gao R, Li C, Ni J, Yang Z, Zhang Q *et al.* Functional assignment of multiple ESCRT-III homologs in cell division and budding in *Sulfolobus islandicus*. *Mol Microbiol*. 2017; 105:540-553.
12. Deng L, Zhu H, Chen Z, Liang YX, She Q. Unmarked gene deletion and host-vector system for the hyperthermophilic crenarchaeon *Sulfolobus islandicus*. *Extremophiles*. 2009; 13:735-46.
13. Martusewitsch E, Sensen CW, Schleper C. High spontaneous mutation rate in the hyperthermophilic archaeon *Sulfolobus solfataricus* is mediated by transposable elements. *J Bacteriol*. 2000; 182:2574-81.
14. Samson RY, Obita T, Hodgson B, Shaw MK, Chong PL, Williams RL *et al.* Molecular and structural basis of ESCRT-III recruitment to membranes during archaeal cell division. *Mol Cell*. 2011; 41:186-96.
15. Wurtzel O, Sapra R, Chen F, Zhu Y, Simmons BA, Sorek R. A single-base resolution map of an archaeal transcriptome. *Genome Res*. 2010; 20:133-41.
16. Peng N, Deng L, Mei Y, Jiang D, Hu Y, Awayez M *et al.* A synthetic arabinose-inducible promoter confers high levels of recombinant protein expression in hyperthermophilic archaeon *Sulfolobus islandicus*. *Appl Environ Microbiol*. 2012; 78:5630-7.
17. Chen L, Brugger K, Skovgaard M, Redder P, She Q, Torarinsson E *et al.* The genome of *Sulfolobus acidocaldarius*, a model organism of the Crenarchaeota. *J Bacteriol*. 2005; 187:4992-9.
18. Liu Y, Osinski T, Wang F, Krupovic M, Schouten S, Kasson P *et al.* Structural conservation in a membrane-enveloped filamentous virus infecting a hyperthermophilic acidophile. *Nat Commun*. 2018; 9:3360.
19. Guo L, Brugger K, Liu C, Shah SA, Zheng H, Zhu Y *et al.* Genome analyses of Icelandic strains of *Sulfolobus islandicus*, model organisms for genetic and virus-host interaction studies. *J Bacteriol*. 2011; 193:1672-80.
20. Sun M, Feng X, Liu Z, Han W, Liang YX, She Q. An Orc1/Cdc6 ortholog functions as a key regulator in the DNA damage response in Archaea. *Nucleic Acids Res*. 2018; 46:6697-6711.